Surface rippling of silica glass surfaces scraped by a diamond indenter

Enrico Gnecco, Jana Hennig,* Elham Moayedi,* and Lothar Wondraczek
Otto Schott Institute of Materials Research (OSIM), Friedrich Schiller University Jena, 07743 Jena, Germany

(Received 14 June 2018; revised manuscript received 7 September 2018; published 5 November 2018)

We report on the formation of regular surface ripples accompanying microscratching of vitreous silica using Berkovich diamond tips. The tips were pulled laterally along the surface with varying normal load of up to 30 mN and scan velocity of up to 500 μm/s. Post mortem AFM analysis and independent confirmation through laser scanning microscopy reveal the occurrence of regular surface ripples in the wear grooves. The average repetition distance of the ripples is in the sub-μm range and increases linearly with the scan velocity. Their corrugation is on the order of a few nm, increasing with the applied load, and well below the indentation depth (of a few hundred nm). The experimental results are interpreted assuming that the tip moves in a stick-slip fashion, while it is elastically driven along the surface. In this framework the static friction to be overcome in the stick phase corresponds to the lateral hardness of the material, whereas the kinetic friction slowing down the tip results from the plowing motion of the latter.

DOI: 10.1103/PhysRevMaterials.2.115601

I. INTRODUCTION

The formation of wavy patterns accompanying the motion of a localized object sliding on a compliant surface is a basic but not clearly understood phenomenon occurring on very different length scales. Examples are the moguls formed in alpine skiing [1], the repeated impressions left in standard scratch tests on polymers and glasses [2,3], and the ripples observed when polymer [4], ionic crystal [5], and semiconductor [6] surfaces are scraped with ultralow normal forces of few tens of nN. The latter phenomenon can be accurately investigated in a variety of controlled conditions (e.g., loading, scan velocity, and temperature) using atomic force microscopy (AFM) only [7,8]. As an example, it has been recently demonstrated that the formation of nanoripples on polymers can be understood as a combined effect of the time-increasing shear stress imposed by the slider (i.e., the sharp probing tip) and the viscoplastic response of the material [9]. In this way the rippling process appears to be ruled by five parameters: normal force F_N, indentation rate dz/dt, scan velocity v, tip geometry, and lateral contact stiffness k. If the indentation pit has a Gaussian cross section of half width σ, surrounded by a circular rim of comparable size, stick-slip motion accompanied by ripples is expected if the inequality $F_N(dz/dt) > k\sigma v$ holds, otherwise the tip will move on continuously. Since the contact area between two solid surfaces sliding past each other usually consists of a multitude of tip junctions which are continuously formed and broken at distinct sites, gaining knowledge on regular wear patterns generated by a single tip, not necessarily on the nanoscale, is crucial for modeling and controlling the response of moving parts of mechanical components, as well as for fundamental aspects.

In this paper we adopt a combination of AFM and nanoindentation techniques to investigate the results of stick-slip motion *in the early stages* of mechanical contact on the surfaces of inorganic glasses with characteristic depth and length scales in sub-μm range. Under these conditions surface deformation is at the origin of material strength and mechanical failure, whereby initial flaws act as stress amplifiers which reduce the applicable strength by several orders of magnitude [10]. To this end we must notice that, while surface scratch tests are routinely performed on glass surfaces, the vast majority of such studies provide only qualitative and empirical information on scratch regimes where significant cracking or abrasion occur [11–14], although formation of patterns with repetition distances of hundreds of μm was also reported in earlier investigations in the high-loading regime [15]. The elastic-plastic regime, on the other hand, has been addressed only recently, following major improvements in nanoindentation technology, from the perspective of grinding performance [16,17] or scratching hardness [18–20]. In this regime, the fundamental relation between stick-slip and topography of the scratch grooves has not been considered thoroughly so far. Here, focusing on the archetype case of vitreous silica, we provide unambiguous evidence and quantitative data on the occurrence of regular surface rippling on silica under concentrated loads of few mN. From the velocity dependence of the ripple repetition rate, we consistently associate this phenomenon to the stick-slip motion of the indenter caused by periodic failure of the glass surface and deceleration of the plowing motion.

II. MATERIALS AND METHODS

The scratch tests and AFM imaging were performed on commercial-grade vitreous silica (Heraues Suprasil 1). A load-controlled nanoindenter (G200, Agilent) equipped with a Berkovich diamond tip was used to generate surface scratches. After a prescanning phase with a loading force below 50 μN,

*These authors have contributed equally to this work.

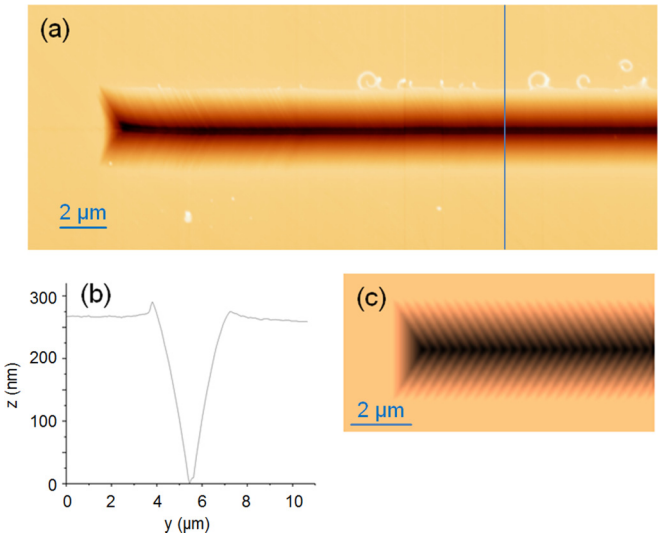

FIG. 1. (a) AFM topography of a silica glass surface previously scratched (left to right) with a normal force of 30 mN and a scan velocity of 10 μm/s. Set point: $F_N = 1.8$ nN. (b) Cross section along the light blue line in (a). (c) Simulated herringbone pattern obtained from the simple repetition of Berkovich geometry every 350 nm without relaxation effects.

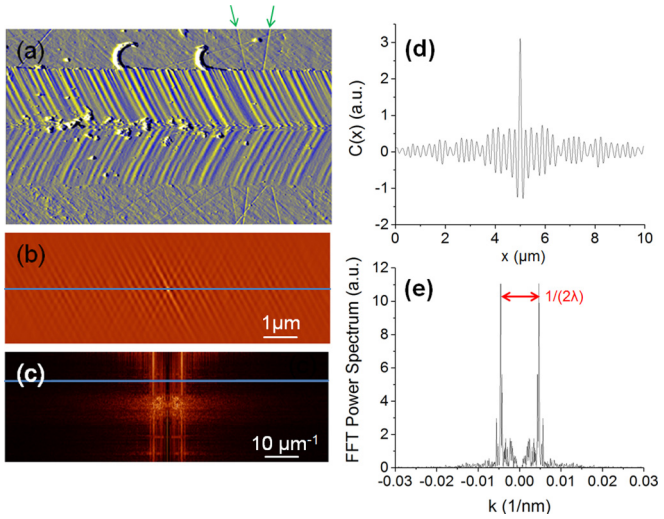

FIG. 2. (a) AFM error signal across the wear scar in Fig. 1(a). The green arrows highlight two polishing lines. Frame size: $10 \times 6\,\mu m^2$; (b) 2D self-correlation and (c) 1D-FFT along longitudinal direction extracted from the region corresponding to the herringbone pattern in (a); (d),(e) cross sections along the blue lines in (b) and (c), respectively.

the tip was suddenly halted and the load was increased up to the chosen setpoint (between 10 and 30 mN, i.e., within the elastic-plastic regime [18]). Scanning was resumed shortly after until the desired scratch length was reached. At this point, the tip was again halted, and the loading force brought back to the prescan value. Together with the penetration depth, the lateral force was recorded during the whole process. The resulting scratch grooves were subsequently imaged using AFM (Nano Wizard 4, JPK Instruments) in contact mode. Silicon nitride probes (Tip B, SNL-10, Bruker) with force constant of 0.12 N/m and resonance frequency of 23 kHz were used, and the fast scan direction was oriented along the scratch direction. All images were analyzed using JPK proprietary software and WSxM 4.0 [21].

III. RESULTS

An AFM image of a typical wear scar on the silica glass surface is shown in Fig. 1(a). The scar has a width of about 3.2 μm and a depth of 250 nm. On the upper edge of the scar a modest pileup of material is observed with width and height of about 300 nm and 20 nm, respectively. A cross section across the scratch groove [Fig. 1(b)] shows that the transverse profile is not perfectly V shaped. The slope increases continuously from 7° to 14° when approaching the axis of the groove. Only the limit value is consistent with the geometry of the Berkovich indenter, which is expected to cut the specimen with an angle α of about 15° with respect to the horizontal plane. As shown in the Supplemental Material [22] (Fig. S1) both width and depth of the scars increase with the normal force F_N, whereas these quantities are not found to change significantly with the scan velocity v.

The accompanying AFM error signal maps [one of which is shown in Fig. 2(a)] clearly reveal the existence of a herringbone pattern across the whole length and width of the scars. The constituent ripples are tilted by 62° with respect to the axis of travel, consistently with the triangular geometry of the Berkovich tip (projected wedge angle of 120°). Several polishing lines, apparently unrelated to the herringbone structure, can also be seen. The repetition distance (period) λ of the ripples is not uniform. The average value of λ can be estimated from 2D self-correlation of the error signal [Figs. 2(b) and 2(d)] or, alternatively, from the 1D fast Fourier transform (FFT) along each horizontal scan line [Figs. 2(c) and 2(e)]. The average values of λ coincide, and FFT allows us to conclude that these values (220 ± 6 nm in the case of Fig. 2) are the same on all longitudinal sections (except for the central region where some impurities are present). As shown in the Supplemental Material [22] (Fig. S2) the ripples can be also recognized in longitudinal sections of magnified topography images. Their period is consistent with the estimation in Fig. 2. Additionally, their rms amplitude is 0.81 nm, corresponding to a corrugation on the order of 2 nm. For reference, ripple occurrence was verified independently by confocal laser scanning microscopy (Zeiss LSM): see Fig. 3.

The scratch test was repeated for six values of v between 10 μm/s and 500 μm/s while keeping F_N at 30 mN. Each scratch groove was imaged at different (nonoverlapping) locations and the average period λ was calculated as described before. As shown in Fig. 4, λ is found to increase almost linearly with v. From linear regression we estimate that $\lambda = \lambda_0 + t_0 v$, with $\lambda_0 = (207 \pm 8)$ nm and $t_0 = (1.07 \pm 0.15)$ ms. This means that the period increases consistently across the range of applied velocities. The corresponding increase of the rms roughness is more irregular—it varies within 0.6 nm and 2.2 nm (not shown).

Additional information was obtained from the time variation of the indentation depth and lateral profiles acquired *in situ* while the nanoindenter was scratching the glass surface.

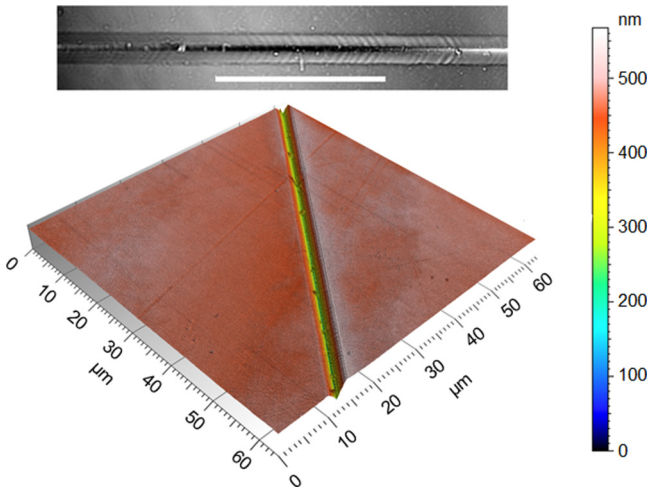

FIG. 3. Laser scanning microscopy image of a wear groove obtained in the same conditions of Fig. 1(a). Scale bar of top view: 20 μm.

As shown in Fig. 5(a) the average depth of the wear groove was $z_0 = 460$ nm, well above the value measured by AFM. Together with the observation that the cross section is not V shaped, we can confirm that the glass significantly recovered during unloading, in line with previous indentation measurements (without scratching) based on Vickers tips [23]. This behavior, which is not observed in other common glasses such as soda-lime silicates, can be attributed to the very open structure of silica glass and the strength of Si-O-Si bonds, facilitating elastic recovery. From the value of the average lateral force $F_L = (4.40 \pm 0.05)$ mN during scratching [Fig. 5(b)] a coefficient of friction $\mu \approx 0.15$ is estimated. This value changes only slightly when the velocity is increased ($z_0 = 475$ nm and $F_L = 4.5$ mN at the maximum value of $v = 500\,\mu$m/s). Noteworthy, the corresponding *in situ* rms value of the indentation depth, 0.87 nm, is only slightly larger than the rms

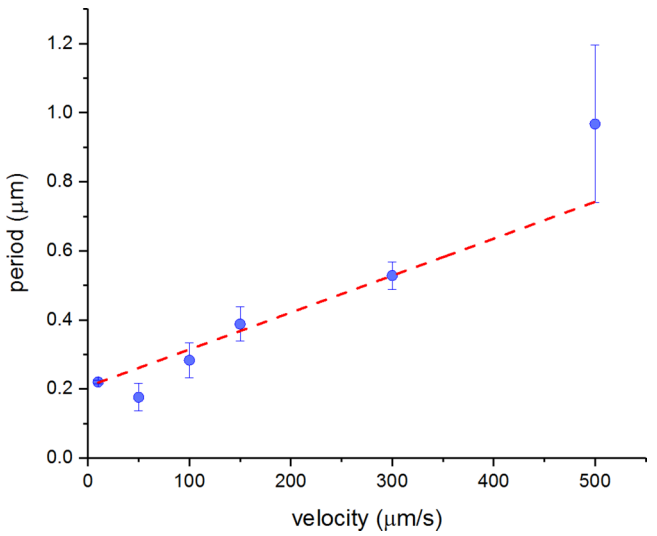

FIG. 4. Velocity dependence of the ripple period as measured by AFM *ex situ* after scratching with a normal force $F_N = 30$ mN (black dots) and linear fit of the experimental data points (red curve).

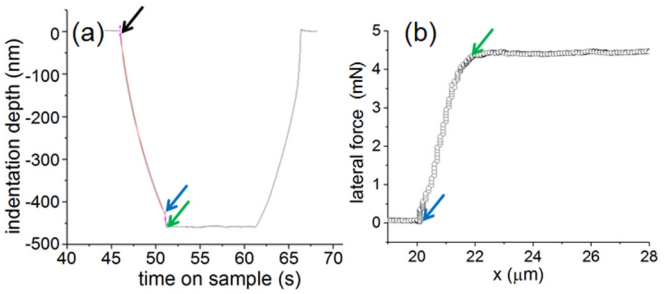

FIG. 5. (a) Time variation of the indentation depth while scratching with $v = 10\,\mu$m/s. Scanning was stopped at the time $t = 46$ s (when the normal load of 30 mN was applied, black arrow) and resumed at $t = 51$ s (blue arrow). A steady state is reached slightly after (green arrow). The red curve is an exponential fit of the data points in this time frame. (b) Lateral force vs indenter position when the scratching process initiates (at $x = 20\,\mu$m). The positions indicated by the blue and green arrows correspond to the times in (a).

value of the ripple profiles after scratching (0.81 nm), and the rms value of the lateral force $\Delta F_L = 0.06$ mN recorded *on line*. Regular variations of these quantities corresponding to the period of the ripple pattern cannot be distinguished with the lateral resolution of the available setup (100 nm). Important for the discussion, the indentation depth increases asymptotically when the normal load is applied [as estimated from the red curve in Fig. 5(a)]. The penetration rate dz/dt is indeed found to change from 175 nm/s [corresponding to the black arrow in Fig. 5(a)] to 50 nm/s (blue arrow), with a characteristic time of 4.3 s. When scanning is resumed (at the point shown by the green arrow) the penetration rate abruptly increases to 250 nm/s for a short time of about 0.2 s. This means that the pressure exerted by the nanoindenter is not balanced by the modified surface profile, and the latter is still evolving when the scratching process begins. Additionally, the lateral force is found to increase continuously when the scan is resumed, as shown by the curve in Fig. 5(b). From the slope of the initial part of this curve an effective lateral stiffness $k = 2.8$ kN/m is estimated. The saturation value of $F_L = 4.40$ mN is reached quickly, within a time frame of 0.2 s.

IV. HERRINGBONE PATTERN AS A RESULT OF STICK-SLIP MOTION

With the information provided by the combined nanoindenter and AFM measurements, we are able to build up a reasonable interpretation for the surface rippling phenomenon so observed. The time spent by the Berkovich tip in each dip of the herringbone pattern is easily estimated as $\lambda/v = 22.0$ ms. During this time, the tip penetrates the surface by an additional depth $\Delta z = (dz/dt)(\lambda/v) = 5.5$ nm at most. This is larger than the corrugation of the ripple pattern, as measured by AFM, which again suggests elastic recovery (with possible relaxation effects). Assuming that the tip apex sticks to an indentation site while the tip is pulled along the x direction with increasing lateral force F_L, a point is eventually reached at which the glass is not able to resist this force and the tip suddenly slips laterally. With a cross-sectional area A of the wear groove of 0.74 μm^2 [as estimated from the scan width

in the AFM images and the indentation depth in Fig. 5(a)] and the lateral force value of $F_L = 4.4\,\mathrm{mN}$ measured in Fig. 5(b), the corresponding hardness $H = F_L/A = 5.9\,\mathrm{GPa}$, in line with recent observations of the lateral hardness of silica [18]. The average energy dissipated in a slip event can be also estimated as $E_{\mathrm{diss}} = F_L\lambda = 0.97\,\mathrm{nJ}$. This value corresponds to breaking of only 6% of chemical bonds in the removed volume $V_{\mathrm{slip}} = A\lambda = 0.163\ \mu\mathrm{m}^3$ (assuming a density $\rho = 2650\,\mathrm{kg/m}^3$ and an average bond energy of 621.7 kJ/mol [24]), suggesting that the ripples are associated to nanofracture processes and not to glass fluidization caused by local heating (which has been reported on larger scales in the context of laser chemical vapor deposition [25]). Interestingly, for regular scratching within the elastic-plastic domain, it has been also reported that the work of deformation which is required for the creation of the permanent scratch groove reaches about one tenth of the corresponding volume energy of silica [18].

To answer the question on what determines the distance traveled by the tip before it stops again, i.e., the ripple period λ, two different assumptions, at least, can be made. At increasing velocities, the tip is expected to indent less deeply the glass surface, reducing the lateral force required to induce the slip. However, one would expect lower values of λ in this case, as observed on polymer surface ripples slightly scraped by AFM [9], but in clear contrast with the results in Fig. 4. This difference is due to the fact that the indenter penetrates the surface much more deeply in the present case, and, as proven by Fig. 5(a), it does not retract much more than 2 nm in the slip phase. The duration t_{slip} of the latter may be also not negligible, as compared to the stick phase duration, t_{stick}. As proven below, this leads to a linear increase of λ with v. To this end let us consider the mechanical response of a rigid object with mass m pulled by a spring with stiffness k along a surface. The sliding is slowed down by a constant kinetic friction force F_k (which, in contrast to more complex numeric models of velocity-controlled stick-slip [26], is simply assumed to be constant) and it becomes possible only if the spring force overcomes a threshold value $F_s\ (>F_k)$, corresponding to the static friction force. Under these general assumptions, it can be proven (see Supplemental Material [22]) that the two phases last for a time

$$t_{\mathrm{slip}} = \frac{2}{\omega_0}\arctan\left(\frac{v_c}{v}\right), \quad \text{and} \quad t_{\mathrm{stick}} = \frac{2v_c}{\omega_0 v}, \tag{1}$$

respectively, where $\omega_0 = \sqrt{k/m}$ is the resonance frequency of the system and $v_c = \omega_0(F_s - F_k)/k$. If $v \ll v_c$ then $t_{\mathrm{slip}} \approx \pi/\omega_0$ and the repetition distance of the stick-slip motion is $\lambda = v(t_{\mathrm{stick}} + t_{\mathrm{slip}}) = \lambda_0 + t_0 v$, where

$$\lambda_0 = \frac{2(F_s - F_k)}{k}, \quad \text{and} \quad t_0 = \frac{\pi}{\omega_0}. \tag{2}$$

This linear response (with initial offset) perfectly matches the experimental results in Fig. 4, after noticing that, in steady conditions, λ is the same as the ripple period. With the values of λ_0 and t_0 from Fig. 4, and k from Fig. 5(b), we can also estimate values of about 0.7 g for the effective mass m of the indenter and 0.28 mN for the difference $\Delta F = F_s - F_k$. The orders of magnitude of both values are consistent with the mass of the stylus terminated by the Berkovich tip and the rms value of F_L while scratching (0.05 mN, comparable to the peak value for a perfect triangular wave). While it is difficult to draw more conclusions on the effective mass m (depending on the nanoindenter design), the discrepancy in the values of ΔF may indicate a smoothing of the transition between stick and slip phases, reducing the lateral force (see Ref. [27] for the observation of this effect in atomic-scale stick-slip measurements). This is also suggested by the blunt features in the herringbone pattern, which, in Fig. 1(c), are compared with the sharper pattern that would result from the simple geometric repetition of the Berkovich profile every 350 nm. In this context it is also interesting to observe that the very end of the scratch, when seen from above, also appears rounded, as showed in the Supplemental Material [22] (Fig. S3). This is a further confirmation of partial surface recovery after scratching.

V. CONCLUSION

In summary, we have demonstrated the occurrence of regular ripple patterns on the surface of a silica glass scraped by a diamond tip with moderate loading forces (up to 30 mN) at different velocities (up to 500 μm/s) and related it to periodic stick-slip motion of the tip. Since most sliding interfaces of technical interest are ultimately formed by a multitude of contact points which are abruptly formed and broken, the information so acquired can be of key interest for understanding much more complex wear processes occurring on the macroscale (and not only on glasses). Specifically, one could expect that not only the irregular time variation of the friction force in a multiasperity sliding contact results from an ensemble of regular stick-slip events, but the accompanying abrasive wear patterns are ultimately caused by overlapping (and possible interference) of 'ripplelike' features similar to those reported here in the rather ideal case of an inverted pyramid vs flat contact. Fourier analysis of the lateral force acquired while scanning may also help to correlate the time evolution of the stick-slip mechanism to the topographical features of the resulting surface patterns.

ACKNOWLEDGMENTS

L.W. acknowledges funding from the European Research Council, ERC Grant No. 681652 (UTOPES). E.M. was supported within the Starting Ramp scheme of Priority Program of the German Science Foundation, "Topological Engineering of Ultra-Strong Glasses" (DFG SPP1594). We thank Susanne Sandkuhl for technical assistance with AFM imaging.

[1] D. A. Lind and S. P. Sanders, *The Physics of Skiing: Skiing at the Triple Point*, 2nd ed. (Springer, New York, 2004).

[2] H. Jiang, Q. Cheng, C. Jiang, J. Zhang, and L. Yonghua, Tribol. Int. **91**, 1 (2015).

[3] T. Y. Kwon, M. Ramachandran, and J. G. Park, Friction **1**, 279 (2013).
[4] O. M. Leung and M. C. Goh, Science **255**, 64 (1992).
[5] A. Socoliuc, E. Gnecco, R. Bennewitz, and E. Meyer, Phys. Rev. B **68**, 115416 (2003).
[6] B. Such, F. Krok, and M. Szymonski, Appl. Surf. Sci. **254**, 5431 (2008).
[7] Z. Elkaakour, J. P. Aime, T. Bouhacina, C. Odin, and T. Masuda, Phys. Rev. Lett. **73**, 3231 (1994).
[8] R. H. Schmidt, G. Haugstad, and W. L. Gladfelter, Langmuir **15**, 317 (1999).
[9] E. Gnecco, P. Pedraz, P. Nita, F. Dinelli, S. Napolitano, and P. Pingue, New J. Phys. **17**, 032001 (2015).
[10] L. Wondraczek, J. C. Mauro, J. Eckert, U. Kühn, J. Horbach, J. Deubener, and T. Rouxel, Adv. Mater. **23**, 4578 (2011).
[11] E. Moayedi and L. Wondraczek, J. Non-Cryst. Solids **470**, 138 (2017).
[12] W. Gu, Z. Yao, and K. Li, Proc. Inst. Mech. Eng., C J. Mech. Eng. Sci. **225**, 2767 (2011).
[13] V. Le Houerou, J. C. Sangleboeuf, S. Deriano, T. Rouxel, and G. Duisit, J. Non-Cryst. Solids **316**, 54 (2003).
[14] W. Wang, P. Yao, J. Wang, C. Huang, T. Kuriyagawa, H. Zhu, B. Zou, and H. Liu, Ceram. Intern. **43**, 10726 (2017).
[15] B. R. Lawn, S. M. Wiederhorn, and D. E. Roberts, J. Mat. Sci. **19**, 2561 (1984).
[16] C. Li, F. Zhang, Y. Di, and L. Liu, Appl. Opt. **55**, 6547 (2016).
[17] H. He, S. H. Kim, and L. Qian, Trib. Int. **94**, 675 (2016).
[18] S. Sawamura, R. Limbach, H. Behrens, and L. Wondraczek, J. Non-Cryst. Solids **481**, 503 (2018).
[19] G. N. B. M. de Macedo, S. Sawamura, and L. Wondraczek, J. Non-Cryst. Solids **492**, 94 (2018).
[20] S. Sawamura and L. Wondraczek, Phys. Rev. Mater. **2**, 092601(R) (2018).
[21] I. Horcas, R. Fernandez, and J. M. Gomez-Rodriguez, Rev. Sci. Instrum. **78**, 013705 (2007).
[22] See Supplemental Material at http://link.aps.org/supplemental/10.1103/PhysRevMaterials.2.115601 for topography images corresponding to Fig. 2(a) and at the very end of the scratch and for derivation of Eq. (1) in the main text.
[23] T. Miura, Y. Benino, R. Sato, and T. Komatsu, J. Eur. Ceram. Soc. **23**, 409 (2003).
[24] P. Jutzi and U. Schubert, *Silicon Chemistry: From the Atom to Extended Systems* (Wiley-VCH, Weinheim, 2003).
[25] R. B. Jackman, J. S. Foord, A. E. Adams, and M. L. Lloyd, J. Appl. Phys. **59**, 2031 (1986).
[26] C. Mathew Mate, *Tribology on the Small Scale* (Oxford University Press, Oxford, 2007).
[27] A. Socoliuc, R. Bennewitz, E. Gnecco, and E. Meyer, Phys. Rev. Lett. **92**, 134301 (2004).